Parametrization of Direct and Soft Steric-Undulatory Forces Between DNA Double Helical Polyelectrolytes in Solutions of Several Different Anions and Cations

Rudi Podgornik,* Donald C. Rau, and V. Adrian Parsegian
NIDDK and DCRT, National Institutes of Health, Bethesda, Maryland 20892 USA

ABSTRACT Directly measured forces between DNA helices in ordered arrays have been reduced to simple force coefficients and mathematical expressions for the interactions between pairs of molecules. The tabulated force parameters and mathematical expressions can be applied to parallel molecules or, by transformation, to skewed molecules of variable separation and mutual angle. This "toolbox" of intermolecular forces is intended for use in modelling molecular interactions, assembly, and conformation. The coefficients characterizing both the exponential hydration and the electrostatic interactions depend strongly on the univalent counterion species in solution, but are only weakly sensitive to anion type and temperature (from 5 to 50°C). Interaction coefficients for the exponentially varying hydration force seen at spacings less than 10 to 15 Å between surfaces are extracted directly from pressure versus interaxial distance curves. Electrostatic interactions are only observed at larger spacings and are always coupled with configurational fluctuation forces that result in observed exponential decay lengths that are twice the expected Debye-Huckel length. The extraction of electrostatic force parameters relies on a theoretical expression describing steric forces of molecules "colliding" through soft exponentially varying direct interactions.

INTRODUCTION

Since realizing the possibility of measuring forces between molecules, by connecting the order in the molecular arrays translated into the intermolecular spacing with the measured osmotic pressure acting on the array, and since discovering qualitative differences from previously expected forces, there has been a need to codify observations to allow practical use of measured forces. Our object in this paper is to create such a "toolbox" for the physical forces between DNA double helices in univalent salt solutions.

Two qualitative features of these forces have now become amply evident: 1) At short separations, less than ~10–15 Å between surfaces, the dominant interaction appears to involve a work of removal of solvent water rather than to indicate an electrostatic or van der Waals interaction acting across a continuous dielectric medium (Leikin et al., 1991, 1993; Rau et al., 1984; Rau and Parsegian, 1992a,b). 2) At larger separations, the onset of macromolecular motion creates mechanical/entropic or "steric" repulsions of much longer range than would be expected from mediating hydration or electrostatic double layer interactions (Podgornik et al., 1989; Podgornik and Parsegian, 1990).

In either regime, the action of salt in the medium is qualitatively different from the simple screening of double layers expected from traditional theories. For example, different cations bound to a negative polyelectrolyte change the hydration properties of the molecular surface and consequently change the strength of the hydration force. To the extent that cations bind with different affinities, there are differences in the residual electrical charge. Different species of anions have only secondary effects on either hydration or steric repulsion. For DNA in the univalent-ion solutions studied here, hydration forces depend only weakly on temperature.

From forces observed between parallel DNA double helices in solutions of five different cations, Li^+, Na^+, K^+, Cs^+, and $N(CH_3)_4^+$ (TMA^+), we have extracted expressions for their hydration and electrostatic double layer repulsion in forms convenient for modelling molecular interactions. In the hope that these simple formulae will permit the assessment of forces in cases where interactions can not be simply inferred from direct measurement on parallel-rod assemblies, we have converted the equations for forces between parallel molecules to what can be felt between skewed rods as a function of separation and mutual angle in solution.

MATERIALS AND METHODS

The experiments examined in this paper have been performed with calf thymus or chicken erythrocyte DNA osmotically stressed with PEG polymer under various ionic conditions and temperatures. The details of the experimental procedures have been described in extenso elsewhere (Rau et al., 1984; Podgornik et al., 1989; Parsegian et al., 1986) and will not be repeated here.

Since in what follows we shall make intensive use of a theoretical model for the analysis of forces in condensed arrays of polymers detailed in reference (Podgornik and Parsegian, 1990), we briefly review the main features of that model. We refer to a simplified (mean-field) picture where each of the polymers in the hexagonal array (as revealed by x-ray diffraction) exhibits configurational fluctuations in an effective tube that mimics the confining action of its neighbors.

A simple expression can be derived under these assumptions

$$W/L = \phi(R)/L + [kT\,l/12\lambda^2]^{1/2}\,[\phi(R)/L]^{1/2}, \quad (1)$$

for the work of interaction, or potential of mean force, per unit length on

Received for publication 6 October 1993 and in final form 20 January 1994.

Address reprint requests to V. Adrian Parsegian, Laboratory of Structural Biology, DCRT, Building 12-A, Room 2041, National Institutes of Health, Bethesda, MD 20892. Tel.: 301-496-6562 (o), 402-4698 (lab); Fax: 301-496-2172; E-mail: vap@cu.nih.gov.

* On leave from J. Stefan Institute, Ljubljana, Slovenia.

0006-3495/94/04/962/10 $2.00

each polymer: a "bare" or direct interaction potential ($\phi(R)/L$) acting between the polymers and the contribution of configurational fluctuations that is coupled to this bare potential, ($[kTl/12\lambda^2]^{1/2}$ $[\phi(R)/L]^{1/2}$). Here R is the radius of the effective tube (or an effective average spacing between the neighbors in the assembly), l is the effective step length introduced by Podgornik and Parsegian (1990) and inferred from experiment (Podgornik et al., 1989), a quantity closely connected with the Odijk deflection length (Odijk, 1986). Its value was experimentally determined as approximately 40 Å (Podgornik et al., 1989). The parameter λ is the effective average exponential decay length of the bare potential, i.e.,

$$\frac{1}{\lambda^2} = \frac{\phi''(R)}{\phi(R)}, \tag{2}$$

where $\phi''(R)$ is the second derivative of the bare potential with respect to the radius of the effective tube.

We now restrict ourselves to considering forces between segments of apposed DNA molecules. The appropriate quantity in this case is the force per unit length $f(D_{int})$ at the interhelical separation $R = D_{int}$. Starting from Eq. 1 for the free energy we can take a spatial derivative for the effective mean force per unit length,

$$f(D_{int}) = f_0(D_{int}) + b\,[f_0(D_{int})]^{1/2}, \tag{3}$$

with $f_0(D_{int})$ the force per unit length corresponding to the bare interaction potential,

$$f_0(D_{int}) = -d(\phi(R)/L)/dR, \tag{4}$$

at $R = D_{int}$. An approximate equation of the same form decoupling the bare and the fluctuation enhanced parts of the interaction can also be obtained for the interaction between planar lipid bilayers (Evans and Parsegian, 1989; Evans, 1991; Podgornik and Parsegian, 1992; Tsao et al., 1993). The coefficient b for the entropic/fluctuation force is given by,

$$b = [kTl/48\lambda^3]^{1/2}, \tag{5}$$

where λ can again be interpreted as an effective exponential decay length. As a point of reference, $b \simeq 2$ (dyne/cm)$^{1/2}$ for $l \simeq 40$ Å (assumed constant over the experimental conditions discussed here) and for the range of decay lengths appropriate for the data considered here.

The relation between osmotic pressure, Π, the experimental variable, and the force per unit length is (Rau et al., 1984),

$$f(D_{int}) = \Pi D_{int}/3^{1/2}. \tag{6}$$

RESULTS

Interhelical separation dependence

Large separations, fluctuation-enhanced double layer repulsion

There is a clear consistency, evident in Fig. 1, in the repulsive forces between DNA double helices in five different 0.4 M salt solutions sharing a common anion (Cl^-). Empirically, the force per unit length varies exponentially with interhelical separation D_{int} and can be written in the form

$$f(D_{int}) = f_{eff}\, e^{-(D_{int}/\lambda_{eff})}. \tag{7}$$

At the large interaxial separations examined in Fig. 1, $D_{int} \geq 30$–35 Å (surface separations greater than $\simeq$10–15 Å), the forces between double helices have *about* the same characteristic decay length λ_{eff} in four cases (Li^+, Na^+, K^+, Cs^+). Only the prefactor f_{eff} differs among these counterions.

What is also clear from the best fitting f_{eff} and λ_{eff} parameters given in Table 1a is that this exponential decay

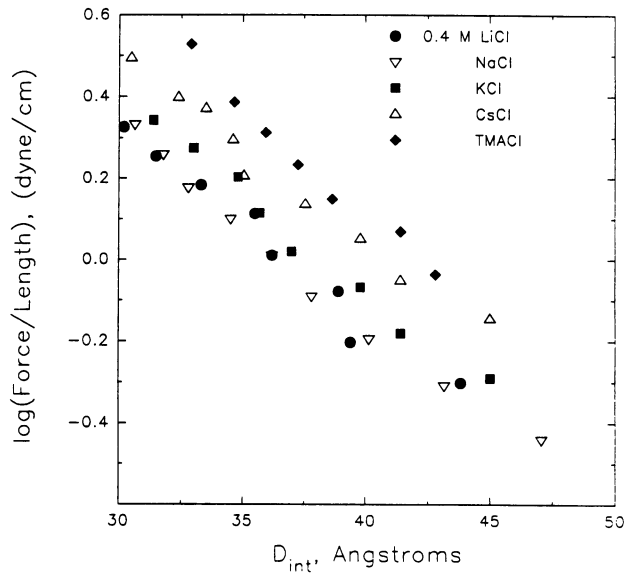

FIGURE 1 Fluctuation-enhanced electrostatic double-layer repulsion between DNA double helices in 0.4 M salt solutions: ●, LiCl; ▽, NaCl; ■, KCl; △, CsCl, diamond TMACl. Forces are plotted as force per unit length (dynes/cm) between parallel helices. The parametrization of the forces in this regime of interhelical spacings D_{int} and osmotic pressures is presented in Table 1a.

length is (to within about 5%) twice the 4.75-Å Debye-Huckel decay length expected from electrostatic double-layer theory. The one exception is for DNA double helices in TMAC1 solutions ($\lambda_{eff}/2 = 4.0$ Å), a system to which we will return specifically below.

It has been shown that this halving of the decay rate correlates with the directly measured, progressive onset of molecular configurational disorder in the helical array, a disorder quantified through the measured width of the interaxial x-ray scattering peak (Podgornik et al., 1989).

The coefficient f_{eff} of this force varies by a factor of two among Li^+, Na^+, K^+, and Cs^+ cations. Since the observed force cannot be described by a straightforward electrostatic double layer model, one cannot relate the variation in force coefficients with the residual charge on DNA helices directly (Stigter, 1975; Manning, 1978; Fixman, 1979, Le Bret and Zimm, 1984; Anderson and Record, 1990).

The mean field model (Podgornik and Parsegian, 1990) of polymers in an array, however, suggests that the observed force per unit length, $f(D_{int})$, acting between the DNA double helices in the array is related to the bare or direct-interaction force, $f_0(D_{int})$ by(Eq. 3, see Methods and Materials above),

$$f(D_{int}) = f_0(D_{int}) + b[f_0(D_{int})]^{1/2}. \tag{8}$$

The square root of the bare force per unit length term is the additional contribution from configurational fluctuations enjoyed by flexible polymers coupled to the potential field. This fluctuation enhanced repulsion will transform an exponentially decaying direct force into another exponential but with twice the decay length of the direct force.

If we approximate the bare electrostatic double layer in-

TABLE 1 Effective force parameters extracted from measurements in the fluctuation-enhanced electrostatic double layer repulsion regime

Salt	[M]	λ_D	$\lambda_{eff}/2$	log (f_{eff})	log(f_{e0})	L_e	ξ
		(Å)	(Å)	(dyne/cm)	(dyne/cm)	(Å)	(Å)
a) The low pressure regime, with interaxial distance D_{int} > 32 Å, at 0.4 M salt							
LiCl	0.4	4.75	4.5	1.69	2.88	3.2	2.2
NaCl	0.4		4.6	1.68	2.86	3.3	2.2
KCl	0.4		4.5	1.76	3.00	2.8	2.5
CsCl	0.4		4.8	1.87	3.22	2.2	3.2
TMACl	0.4		4.0	1.95			
b) The low pressure regime at different NaCl concentrations							
NaCl	0.2	6.7	6.6	1.32	2.59	2.6	2.7
	0.3	5.5	5.6	1.50	2.73	2.9	2.4
	0.4	4.75	4.6	1.68	2.86	3.3	2.2
	0.6	3.9	3.8	1.97	3.19	3.4	2.1

The parameters above were extracted from Fig. 1 (Table 1a) and Fig. 2 (Table 1b). λ_{eff} was determined from a direct fit of the curves to an exponential force, $f(D_{int}) = f_{eff} \exp(-D_{int}/\lambda_{eff})$. Except for the TMA salt, the effective decay length was always very close to twice the expected Debye decay length, λ_D. Effective force coefficients, f_{eff}, were calculated using a decay length $\lambda_{eff} \cong 2\lambda_D$ (6). Bare electrostatic force coefficients, f_{e0}, were calculated from f_{eff} values using Eq. 11 with b calculated from Eq. 5 with $\lambda = \lambda_D$ and the experimentally measured step length 1 = 40 Å (6). The equivalent linear charge density parameters, L_e and ξ, were determined from the f_{e0} values using a linearized Poisson-Boltzmann equation described in the text. These quantities can be introduced directly into the following relations:

potential of mean force per unit length: $W_e(R)/L = f_{e0}\,\lambda_D e^{-R/\lambda_D}$

force per unit length between parallel rods: $f_e(R) = f_{e0}e^{-R/\lambda_D}$

energy of interaction between skewed rods: $W_{skewed}(R, \vartheta) = (f_{e0}\lambda_D^2/\sin\vartheta)(2\pi R/\lambda_D)^{1/2}e^{-R/\lambda_D}$,

where R here is the *minimum* distance between axes of the skewed rods and ϑ is the angle between these axes (viewed along R) (Brenner and Parsegian, 1974).

teraction as an exponential,

$$f_0(D_{int}) = f_0^{el}(D_{int}) = f_{e0} \exp(-D_{int}/\lambda_D), \qquad (9)$$

with λ_D = 4.75 Å (the Debye shielding length of a 0.4 M univalent ion solution), then the data in Fig. 1 can be fit to Eq. 8 with only the electrostatic force magnitude, f_{e0}, for each cation type as a variable. Within the observed force per unit length regime of Fig. 1, only the fluctuation-enhanced repulsion contributes significantly. The extracted f_{e0} magnitudes are given in Table 1a, and range from $\sim 10^{2.9}$ for Li^+ and Na^+ to $\sim 10^{3.2}$ dyne/cm for Cs^+.

This electrostatic amplitude of the interaction potential can be related to the net electrostatic charge density along a single DNA helix through Poisson-Boltzmann theory. (In this formulation we have recognized the result of Manning (1978) that on physical grounds alone the residual potential on the ion-condensed polymer surface is on the order of kT/e or 25 mV. At the interaxial spacings where we observe electrostatic interactions, one can then use a linearized Poisson-Boltzmann equation to good approximation to compute the electrostatic potential whose interactions compress the physically important molecular undulations.)

To put our results in familiar language, we can define L_e as the axial separation between effective or equivalent charges along the DNA molecule where these charges are assumed to reside uniformly distributed on a smooth cylinder of radius a (=10 Å). Then (e.g., Brenner and Parsegian (1974))

$$f_{e0} = \frac{2kTL_b(2\,D_{int}/\pi\,\lambda_D)^{1/2}}{\{\lambda_D\,[L_e(a/\lambda_D)K_1(a/\lambda_D)]^2\}} \qquad (10)$$

where L_b is the Bjerrum length ($=e^2/\epsilon kT$), and $K_1(x)$ the first order cylindrical Bessel function. The reduced charge density parameter ξ widely used in counterion condensation formalism is simply given by L_b/L_e. This formulation incorporates the large-argument approximation of the $K_0(D_{int}/\lambda_D)$ Bessel function as an exponential, $(2D_{int}/\pi\lambda_D)^{-1/2} \exp(-D_{int}/\lambda_D)$.

Values of L_e and ξ extracted by this indirect procedure are displayed in Table 1. Not only does DNA appear more highly charged than expected from counterion condensation ($\xi > 1$), but there is also a significant dependence on counterion type, reflecting the relative adsorption of different cations to the DNA surface. Values of L_e range from 3.3 Å (ξ = 2.2) for Na^+ to 2.2 Å (ξ = 3.2) for Cs^+.

The influence of the salt concentration on the force characteristics can be assessed from the data in Fig. 2, spanning the NaCl concentration range from 0.2 to 0.6 M. Once again, the observed exponential decay length is very close to twice the expected Debye shielding length. We fit these data considering only the dominant fluctuation enhanced repulsion with electrostatic interaction as underlying bare potential, i.e.,

$$f(D_{int}) \cong b[f_0^{el}(D_{int})]^{1/2}. \qquad (11)$$

We assume the electrostatic force, $f_0^{el}(D_{int})$, can again be approximated by Eq. 9 and take the decay length to be the Debye length, λ_D. The extracted net charge density parameters are given in Table 1b. A significant dependence of the reduced surface charge density on ionic strength is apparent. The effective charge density decreases by about 30% between 0.2 and 0.6 M NaCl.

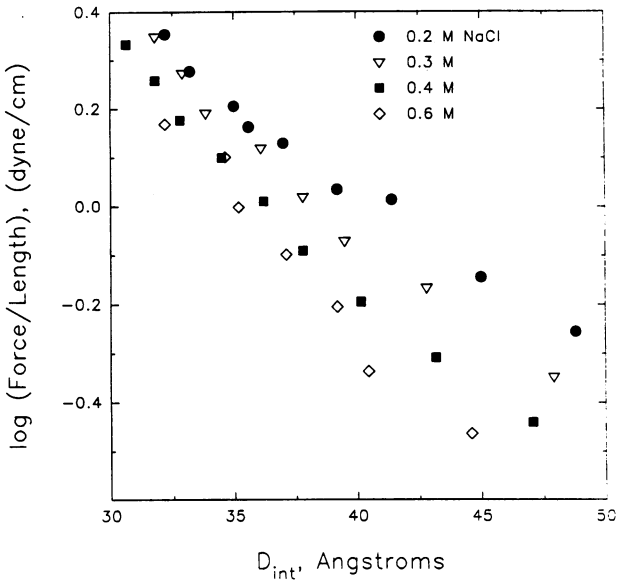

FIGURE 2 Fluctuation-enhanced electrostatic double-layer repulsion between DNA in NaCl solutions of different concentration. ●, 0.2 M; ▽, 0.3 M; ■, 0.4 M; ◇, 0.6 M. Forces are again plotted as force per unit length (dynes/cm) between parallel helices. The parametrization of the forces in this regime of interhelical spacings and pressures is presented in Table 1b.

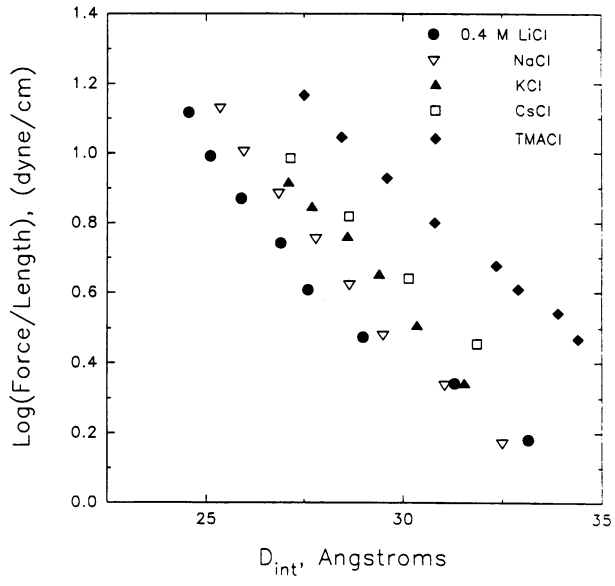

FIGURE 3 Sensitivity of hydration force repulsion in the large pressure regime to cation type. DNA double helices in 0.4 M solutions: ●, LiCl; ▽, NaCl; ▲, KCl; □, CsCl; ◆, TMACl. Forces are again plotted as force per unit length (dynes/cm) between parallel helices. The parametrization of the forces in this regime of interhelical spacings and pressures is presented in Table 2a.

Hydration repulsion at small separations

There is now ample evidence (Leikin et al., 1993) that hydration forces dominate the interaction between many different kinds of polar biopolymers at surface separations less than ≈10–15 Å. Repulsion between double helices converges to an exponentially varying function with an apparent decay length of about 3.0–3.5 Å for 0.1 to 1.0 M NaCl solutions (Rau et al., 1984). The force coefficient depends on the kind of counterion in solution, but not on its concentration. The absence of pronounced sensitivity of decay lengths and force magnitudes to ionic strength means these forces in the high pressure regime exhibit no double layer electrostatic effects. The interaction is dominated by hydration forces. These so strongly overwhelm any residual electrostatic effects that charge contributions are simply not seen at these pressures. Because in this regime the widths of the x-ray diffraction peaks are insensitive to applied Π_{osm} and D_{int}, we assume that the strength of the confining potential is so large that the configurational fluctuations are effectively suppressed.

Fig. 3 shows high pressure data in 0.4 M salt for LiCl, NaCl, KCl, CsCl, and TMACl. Table 2a summarizes the bare exponential force parameters we extract from directly fitting this data, the force coefficient, f_{h0}, and decay length, λ_h. There is a systematic variation of decay length with force magnitude (from 3.0 Å for Li^+ to 4.0 Å for TMA^+) that may reflect deviations from pure exponential behavior at these close separations due to the cylindrical geometry of the DNA array. While the variation of the bare hydration force decay rates is an important issue in itself (Kornyshev and Leikin, 1989), our concern here is primarily to tabulate force parameters. Given the differences in decay lengths λ_h, the extrapolated coefficients f_{h0} do not by themselves indicate differences in the magnitude of hydration forces with different counterions within the range of measured distances.

Fluctuation-enhanced hydration forces, large separation

We now pass in Fig. 4 to the low pressure regime for interactions measured in 2.0 M solutions, a concentration with a Debye length (2.1 Å) that is significantly shorter than the hydration force decay length. The measured decay lengths, $\lambda_{eff} \sim 6.4$ to 7.9 Å, (given in Table 2b) are about twice the value of the decay length observed for bare hydration forces at high pressures ($\lambda_h \sim 3.0$–4.0 Å, Table 2a). They are very unlike a 2.1-Å expected Debye length or a 4.2-Å fluctuation enhanced electrostatic decay length.

Following the observation that $\lambda_{eff} \simeq 2\,\lambda_h$, we interpret λ_{eff} in terms of a fluctuation enhanced hydration repulsion that should ideally show a factor-of-two difference in the decay length (Podgornik et al., 1989; Podgornik and Parsegian, 1990). We again use Eq. 8 to extract a direct or bare hydration interaction $f_0(D_{int})$ from the observed $f(D_{int})$ with its additional configurational fluctuation contribution.

In the same way that we interpreted the low pressure data for double layer forces as being entirely a fluctuation-enhanced repulsion, we here also extract bare hydration force magnitudes by fitting the data in Fig. 4 to

$$f(D_{int}) = b(f_{h0}\, e^{-(D_{int}/\lambda_h)})^{1/2}. \quad (12)$$

The bare force parameters extracted from the data are summarized in Table 2b.

TABLE 2 Effective force parameters extracted from measurements in the bare and fluctuation-enhanced hydration repulsion regime

Salt	Conc	λ_h	$\log(f_{h0})$
	[M]	(Å)	(dyne/cm)
a) High pressure, D_{int} < 32 Å			
LiCl	0.4	3.0	4.64
NaCl	0.4	3.1	4.65
KCl	0.5	3.35	4.48
CsCl	0.4	3.7	4.16
TMACl	0.4	4.0	4.12

Salt	Conc	λ_{eff}	λ_h	$\log(f_{eff})$	$\log(f_{h0})$
	[M]	(Å)	(Å)	(dyne/cm)	(dyne/cm)
b) Low pressure, D_{int} > 32 Å					
LiCl	2.0	6.4	3.2	2.05	3.09
NaCl	2.0	7.1	3.6	2.03	3.20
KCl	2.0	7.9	3.9	2.01	3.27
TMACl	2.0	7.5	3.7	2.28	4.01
TMACl	0.4	7.8	3.8	1.95	4.24

The parameters above were determined for the data in Fig. 3 (Table 2a) and Fig. 4 (Table 2b). At high pressures, values of λ_h and f_{h0} were extracted from a direct fit of the curves to an exponential form for the force, $f(D_{int}) = f_{h0} \exp(-D_{int}/\lambda_h)$. A force curve at 2 M CsCl could not be obtained due to a very high intensity in background scattering for this salt. In the small pressure regime we have again (see Table 1) $f_{eff} = b[f_h]^{1/2}$ and $\lambda_{eff} = 2\lambda_h$, where λ_h given in the table has also been used to obtain b using the relation Eq. 5:

potential of mean force per unit length: $W_h(R)/L = f_{h0}\lambda_D e^{-R/\lambda_h}$

force per unit length between parallel rods: $f_h(R) = f_{h0}e^{-R/\lambda_h}$

force between skewed rods:

$$W_{skewed}(R, \vartheta) = (f_{h0}\lambda_D^2/\sin\vartheta)(2\pi R/\lambda_h)e^{-R/\lambda_h}.$$

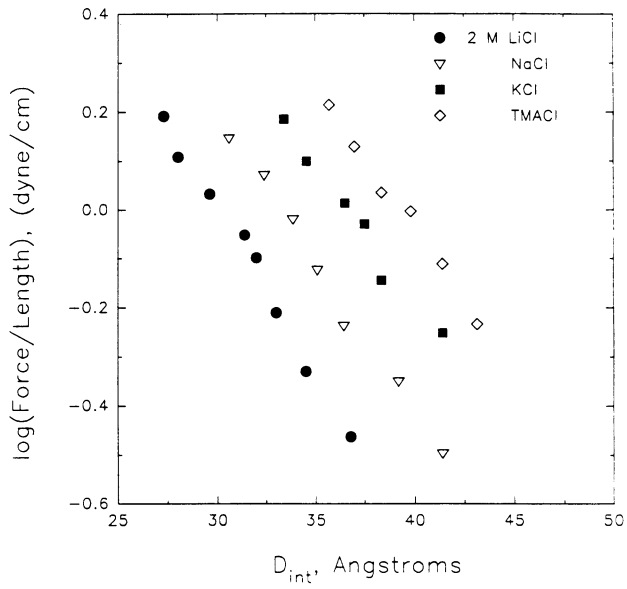

FIGURE 4 Fluctuation-enhanced hydration repulsion between helices in 2.0 M solutions: ●, LiCl; ■, NaCl; ▽, KCl; ◇, TMACl. Forces are again plotted as force per unit length (dynes/cm) between parallel helices. The parameterization of the forces in this regime of interhelical spacings and pressures is presented in Table 2b. In all cases, the apparent decay length is about twice the direct hydration force (Fig. 3) decay length (Table 2a). In 2.0 M solutions, the electrostatic double layer repulsion is expected to be screened by a λ_D = 2.1-Å Debye length. This is much less than the $\lambda_h \cong$ 3.0–4.0 Å for the hydration forces which now dominate electrostatic interactions at all separations.

Bare hydration force coefficients calculated in the fluctuation enhanced, low pressure regime for Li^+ and Na^+ DNA are significantly different from their corresponding values directly extracted from high pressure data (Table 2a).

A transition between the high pressure, bare hydration dominated and low pressure, fluctuation enhanced force regimes occurs at about 30–35 Å and is characterized by a relatively sharp break in the Na^+ and Li^+ force curves (see, for example, Fig. 8 of Podgornik et al. (1989)). The transition is much more abrupt than predicted by Eq. 8. Yet the factor-of-2 difference in decay lengths between the high and low pressure regions indicates a well defined change from fluctuation enhanced hydration repulsion to bare hydration forces. We do not understand the reason for this sharp transition or (and perhaps related) the discrepancies between the high and low pressure estimates of f_{h0} for Li^+ and Na^+ DNA. It may be a concomitant of the hexagonal-cholesteric phase transition reported by Durand, Doucet, and Livolant (Livolant, 1991; Durand et al., 1992) that appears to occur between the two force regimes.

TMA chloride solutions

If we now plot in Fig. 5 all the extracted $f_0(D_{int})$ results for the 0.4 and 2.0 M TMACl solutions obtained at both low (essentially only fluctuation enhanced hydration repulsion) and high pressures (where only the bare hydration force is apparent), we see that all data sets collapse onto approximately a single line with a decay length of about 3.9 Å.

The forces in 0.4 M TMACl, however, tell us more. In both pressure regimes, the force is basically hydration dominated, be it in its bare form or in its fluctuation enhanced form. For TMACl-DNA the hydration force is so powerful (Fig. 3) that it seems even to dominate the electrostatic interactions that appear at low pressures with other cations (Figs. 1 and 2). The exponential decay length and force coefficient at low pressure is insensitive to TMACl concentration between at least 0.4 and 2.0 M. As with the other univalent counterions, a somewhat abrupt transition between bare and fluctuation enhanced forces seems to occur between 30 and 35 Å. Unlike the cases of DNA in Na^+ and Li^+ solutions, however, there is fairly close agreement between bare hydration force coefficients calculated from high and low pressure data with TMA^+.

Temperature dependence of Na-DNA forces

One immediate mental association with any solvation force is the implied role of entropy of solvent release from the molecular surface. Since the integral of a force versus separation is a work or free energy and since the temperature derivative of a free energy is an entropy, the entropic part of a force can be measured from its temperature sensitivity. Indeed, hydration forces can be quite sensitive to temperature. It has recently been possible to measure the entropy and enthalpy versus separation between DNA double helices in divalent Mn^{2+} solutions (Leikin et al., 1991).

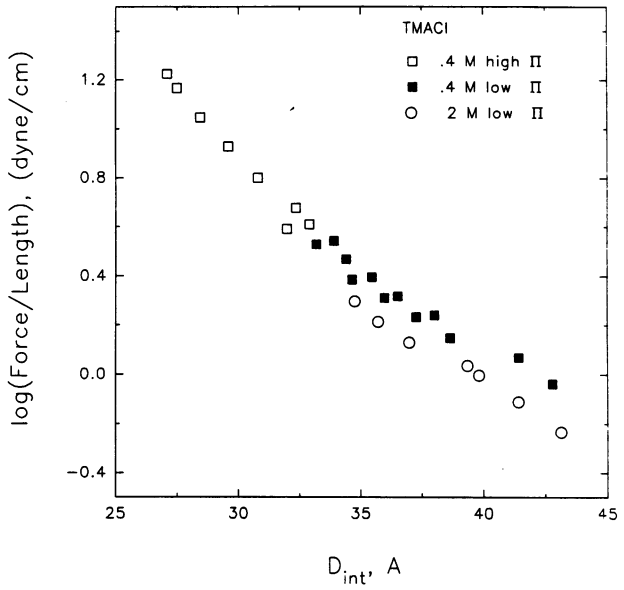

FIGURE 5 The construction of the bare interaction force for TMA salt at 0.4 and 2 M concentration. The raw data in the small and large force regime (corresponding to large and small interhelical spacings) were taken from Figs. 3 and 4. The bare potential in the high pressure regime, $D_{int} < 30$–32 Å, was assumed to be equal to the measured potential. For the bare potential in the fluctuation enhanced regime the relation between the bare and the total force per unit length was taken in its inverse form $f_0(d_{int}) \simeq [f(d_{int})/b]^2$ (see main text). The extracted bare potential in the case of 0.4 M as well as 2 M TMACl both sets of data now collapse to approximately the same straight line with $\log(f_0^{eff} \simeq 4.1$ and $\lambda_{eff} \simeq 3.7$ Å. For the TMA salt (where electrostatic effects are essentially absent), we are thus able to extract a bare potential in the whole range of interhelical spacings probed in the experiments.

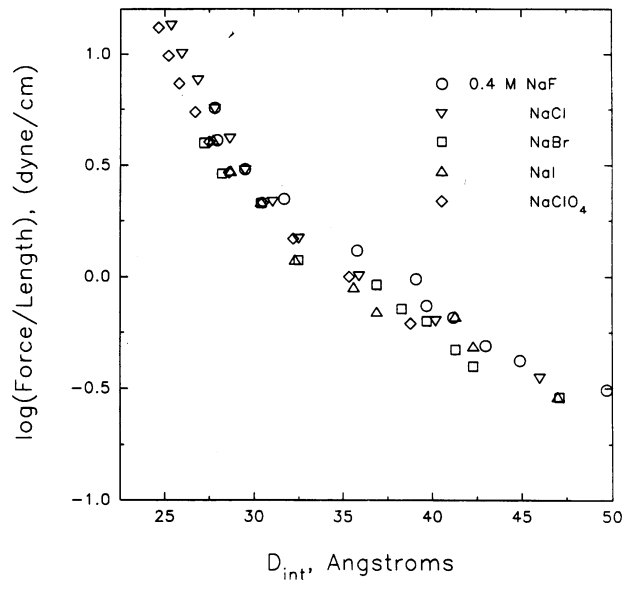

FIGURE 6 The weak effect of anion type on both hydration and electrostatic double layer repulsion between Na^+-DNA double helices. Force per unit length measured in 0.4 M solutions: ○, Na F; ▽, Na Cl; □, Na Br; △, Na I; and ◇, $NaClO_4$.

The temperature dependence of the force between DNA double helices in 0.5 M NaCl is shown in Fig. 7. Higher temperatures give slightly stronger forces.

Examination of the differences in forces measured at different temperatures shows that entropy and free energy (work) are of the same sign and of a comparable order of magnitude and that the absolute magnitude of the entropic contributions is similar to what is seen in Mn^{2+}-DNA arrays. The temperature dependence of the Mn^{2+}-DNA forces is more prominent since enthalpy and entropy are of opposite sign and about equal magnitude and the free energy an order of magnitude smaller. The entropies of solvent release are of opposite sign for Na^+-DNA versus Mn^{2+}-DNA, perhaps because there can be net attraction between Mn^{2+}-DNA but strong repulsion between Na^+-DNA double helices. These matters will be deferred for more careful later study.

Forces measured in solutions of different anions

In qualitative contrast to the case for positive ions, the forces between DNA molecules in various Na^+ salts are but slightly dependent on anion species, Cl^-, I^-, Br^-, F^-, and ClO_4^- (Fig. 6). Hence, there is no sign that anions interact with the DNA molecule to affect significantly either net charge or strength of hydration. The small effect of anions observed is consistent with the Hofmeister series. Water structure breaking, "chaotropic" anions like ClO_4^- or I^- give weaker forces, while water structure makers like F^- strengthen the force. This is qualitatively similar to the anion effects seen with Mn^{2+}-DNA that were ascribed to changes in bulk water entropy that modulate the total entropy of solvent release. As with the temperature dependence seen in Fig. 7, the magnitude of the anion effect seen here is consistent with the magnitude of the anion effect for Mn^{2+}-DNA.

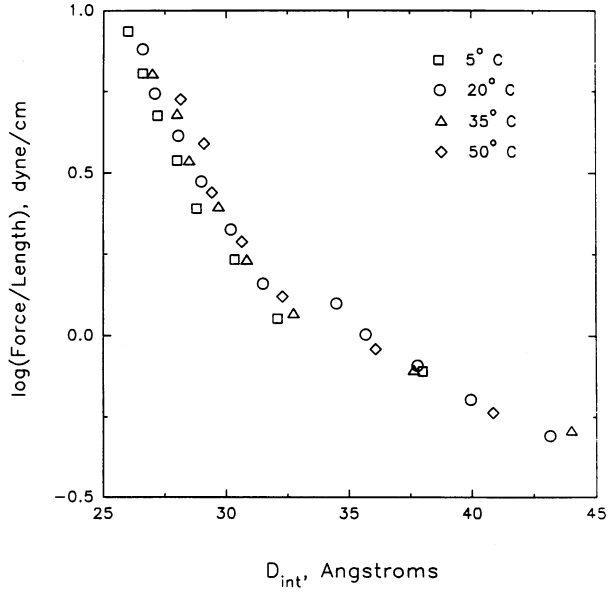

FIGURE 7 Temperature dependence of the hydration and the electrostatic double layer repulsion between Na-DNA helices in 0.4 M NaCl solutions. $T = 5$°C (○), 20°C (□), 35°C (△), and 50°C (◇).

Practical formulae, a toolbox for using measured forces

Measurements seem to give a consistent picture of DNA-DNA interactions in condensed arrays with local hexagonal packing symmetry. This is, however, not always the geometric arrangement between DNA molecules whose interactions one might like to estimate for various situations. Therefore, we have derived several approximate relations or "force extrapolation formulae" that provide accurate, experimentally based estimates of the forces between DNA molecules not only tightly packed into an array but also between freely suspended helices in dilute solutions.

For simplicity, and without loss of experimental accuracy, we write the underlying "bare" interaction potential ($f_0(R)$) acting between the helices as though the molecules were in one or the other of the hydration or electrostatic regimes. One conveniently assumes the forms

$$f_0^{\mathrm{hyd}}(R) = f_{\mathrm{h0}} \exp(-R/\lambda_{\mathrm{h}}) \tag{13}$$

or

$$f_0^{\mathrm{el}}(R) = f_{\mathrm{e0}} \exp(-R/\lambda_{\mathrm{D}}) \tag{14}$$

with λ_{h} and λ_{D} standing for the bare hydration and the Debye decay lengths. Here we use a form of the hydration force potential appropriate for separations larger than the decay length; a better form might be used after one has a consistent theoretical description of the hydration force at very small separations.

We shall consider three different regimes that differ in terms of the relative importance of hydration and electrostatic forces as well as in their fluctuation enhanced modifications.

Stiff parallel rods when fluctuations give no appreciable contribution to the total interaction

This would occur, for instance, when one wants the forces between single DNA fragments in solution. The total force per unit length between two fragments assumes the form

$$f(R) \simeq f_{\mathrm{h0}} \exp(-R/\lambda_{\mathrm{h}}) + f_{\mathrm{e0}} \exp(-R/\lambda_{\mathrm{D}}). \tag{15}$$

The force magnitudes (f_{h0}, f_{e0}) in this case are given in Tables 1 and 2. The same extracted parameters for the force per unit length are appropriate for the calculation of the interaction energies and torques between two skewed fragments of DNA (below).

In a condensed ordered phase where configurational fluctuations dominate

Recalling that disorder couples with the forces acting between helices, the appropriate form of the force per unit length is

$$f(R) \simeq b[f_0]^{1/2} \exp(-R/2\lambda), \tag{16}$$

where both f_0 as well as λ can now refer to the hydration enhanced (large salt) regime with $f_0 = f_{\mathrm{h0}}$ and $\lambda = \lambda_{\mathrm{h}}$, or to the electrostatic enhanced (low salt) regime $f_0 = f_{\mathrm{e0}}$ and $\lambda = \lambda_{\mathrm{D}}$. The connection between f_{e0} and the charge per unit length of the DNA helix treated as an equivalent charged cylinder is in this case

$$f_{\mathrm{e0}} = \frac{2kTL_{\mathrm{b}}\,(2R/\pi\lambda_{\mathrm{D}})^{1/2}}{\{\lambda_{\mathrm{D}}\,[L_{\mathrm{e}}(a/\lambda_{\mathrm{D}})\,K_1(a/\lambda_{\mathrm{D}})]^2\}}. \tag{17}$$

For fluctuation enhanced electrostatic dominated forces, one can thus write finally

$$f(R) \simeq \frac{b[2kTL_{\mathrm{b}}/\lambda_{\mathrm{D}}]^{1/2}\,[2R/\pi\lambda_{\mathrm{D}}]^{1/4}}{[L_{\mathrm{e}}(a/\lambda_{\mathrm{D}})K_1(a/\lambda_{\mathrm{D}})]} \exp\left(-\frac{R}{2\lambda_{\mathrm{D}}}\right). \tag{18}$$

The conspicuous characteristic of the form of the force per unit length of the DNA helix in this case is a linear (instead of a quadratic) dependence on the amount of charge residing on the backbone. These charge densities, as equivalent linear charge density on a 10 Å radius cylinder, are shown in Table 1.

Forces between skewed rods

Knowledge of forces operating between parallel rodlike molecules can now be used to assess the interaction between skewed rods interacting at a minimal interaxial separation R and at a mutual angle (of rotation from parallel configuration) ϑ. Writing the interaction energy of two parallel rods at a separation R per unit length of the rod ($W(R)/L$) in the form,

$$W(R)/L = (f_{\mathrm{e0}}\lambda_{\mathrm{D}})\exp(-R/\lambda_{\mathrm{D}}), \tag{19}$$

then using pairwise summation, the total interaction between two thin skewed rods can be obtained via an integral over the whole length (see Brenner and Parsegian (1974)),

$$\begin{aligned} W_{\mathrm{skewed}}(R, \vartheta) &= \int_{(L)} \frac{W(r(l))}{L}\, dl \\ &\simeq \frac{f_{\mathrm{e0}}\lambda_{\mathrm{D}}^2}{\sin\vartheta}\left(\frac{2\pi R}{\lambda_{\mathrm{D}}}\right)^{1/2} \exp\left(-\frac{R}{\lambda_{\mathrm{D}}}\right), \end{aligned} \tag{20}$$

where $r(l)$ is the local perpendicular distance between the skewed rod-like molecules at position l along one of them (for easier visualisation of the geometric arrangement in the above integral see Brenner and Parsegian (1974)), while R is now the minimal separation between rods. The above approximate form of the integral is valid for the case when the Bessel function of order 1 can be approximated by its asymptotic form. It is clear that the interaction energy for skewed rods varies slightly more slowly with separation then is the case for parallel rods. On the other hand for $\vartheta = 0°$ (parallel rods) the total interaction energy becomes infinite for infinite rods and scales linearly with rod length. The energy per unit length remains finite, as indeed it should.

When does the difference between the energies for parallel (Eq. 15, $\vartheta = 0°$) and crossed (Eq. 20, $\vartheta = 90°$) configurations of two interacting DNA molecules become comparable to the thermal energy? Consider

$$kT \simeq L\left[\frac{W(R)}{L}\right] - W_{\text{skewed}}(R,90°) \tag{21}$$

$$= L_0(f_{e0})\exp(-R\lambda_D) - (f_{e0}\lambda_D^2)\left(\frac{2\pi R}{\lambda_D}\right)^{1/2}\exp\left(-\frac{R}{\lambda_D}\right),$$

or equivalently

$$L_0/\lambda_D - (2\pi R/\lambda_D)^{1/2}) \simeq (kT/f_{e0}\lambda_D^2)\exp(R/\lambda_D), \tag{22}$$

where L_0 is the rod length. Recalling now the measured values for f_{e0} and λ_D (in Table 1), one obtains that for all measured cases $(kT/f_{e0}\lambda_D^2) \ll 1$ while $\exp(R/\lambda_D) \gg 1$.

For long molecules, with $L_0 \gg R$, one can drop the $-(2\pi R/\lambda_D)^{1/2}$ term to obtain,

$$(R/\lambda_D) \simeq \ln(L_0/\lambda_D) - \ln(kT/f_{e0}\lambda_D^2). \tag{23}$$

Taking now two DNA segments in 0.2 M NaCl salt (physiological conditions) 500 Å long, comparable to the persistence length of the native DNA or the total length of a nucleosomal DNA fragment, we obtain an interaxial separation R close to 40 Å for the distance at which the energy difference between the two limiting geometrical arrangements is 1 kT.

DISCUSSION

We have analyzed forces measured in arrays of DNA double helices and have derived formulae to be used to describe molecular interactions in solution. We offer these results with the caveat that must go with any attempt to describe precisely what is still not well understood physically. The insensitivity of DNA force curves at high pressures to bulk salt concentration and the close similarity of stress versus distance curves measured at high osmotic pressure for materials as diverse as lipid bilayers, DNA, several stiff polysaccharides, and collagen (Leikin et al. (1993), and references therein) has forced us to postulate hydration forces. Exponentially varying forces at close separation are seen for systems that are highly charged, moderately charged, net neutral, and wholly uncharged. The binding and structuring of water by polar surfaces seems to be the only common characteristic.

Over the entire range of interhelical spacings, the measured forces between DNA helices in ordered arrays are repulsive in univalent salt solutions. There is no indication of any abrupt decrease in spacing over a narrow pressure range that is expected for an attractive force of a magnitude that is significant compared to the observed repulsion and that has been seen for DNA with several divalent and most all multivalent counterions (Rau and Parsegian, 1992*a*, *b*). An attractive interaction that is much weaker than the observed repulsion, such as a van der Waals force or an ionic fluctuation force (Wang and Bloomfield, 1991), would, of course, not be seen.

Without a rigorous theory, it is enough to write the simplest functions that describe the data. The formulae given for hydration interactions or confined fluctuations are only approximate and empirical. We have written a single exponential for the direct hydration or electrostatic double layer interaction. For even greater simplification, we have analyzed the forces measured in arrays as though only one or the other of these interactions is operating at a particular separation.

In each regime, high versus low osmotic stress, high versus low salt concentrations, temperatures from 5 to 50°C, several kinds of univalent cations and anions, the extracted formula seem to give satisfactory account of the forces.

Contrary to conventional wisdom, in no pressure regime do direct electrostatic double layer interactions satisfactorily describe the observed interactions between charged DNA double helices. At close separations, hydration dominates. At larger separations, these forces couple with molecular motion to create interaction free energies that resemble neither the pure electrostatic force nor the steric undulatory forces with which they are blended. It is not easy to separate the interhelical potential from changes in the configurational freedom of DNA without careful examination of both interaction free energy and molecular disorder.

The observed interaction free energy and the derived force per unit length at large separations are dominated by entropic forces, originating in the quenched configurational fluctuations of the polymers in the array. The quenching is provided mostly by the soft electrostatic or hydration interaction potential, probably not at all by the steric hard collisions (Podgornik et al., 1989; Podgornik and Parsegian, 1990). In contrast to conventional theories for calculating confinement entropies that use square well or hard core potentials to approximate electrostatic interactions, Eq. 3 incorporates a more realistic spatially varying potential. The simple doubling of the expected Debye shielding length experimentally observed is a direct consequence of keeping the whole exponentially varying potential and not simplifying it by creating an effective hardcore or step potential. The step length, l, in Eq. 5 that characterizes the configurational freedom in the absence of soft interhelical forces is wholly derived from the experimentally measured variation in the width of the interhelical x-ray scattering peak. These peak widths are sensitive indicators of molecular disorder. Now that they have been measured (Podgornik et al., 1989) they can be used to assess the validity of theories describing fluctuations with several fitting parameters, rather than the soft potentials used by us. In a recent study Odijk (1993) develops a mean-field theory for the interplay of configurational fluctuations and forces in hexagonal arrays of stiff polymers. The major improvement in this work over (Podgornik and Parsegian, 1990) is that a self-consistent estimate for the effective steplength, comparable with the experimentally observed parameter, is now derived explicitly.

The DNA molecule seems about half neutralized ($\xi \sim$ 2–2.5 for NaCl), far less than expected from ion condensation theory, but the extent of neutralization does change with the kind of cation in the suspending medium. These numbers can be compared with estimates available in the literature based on numerical solution of the Poisson-Boltzmann equation. The reduced effective charge (ξ) density calculated for isolated DNA helices modelled as a smooth 10-Å radius cylinders and for 0.4 M salt (assumed point charges) is about 2.9 (Stigter, 1975; Fixman, 1979; Le Bret and Zimm, 1984). This is the effective reduced charge density on DNA as seen from "infinitely" far away. Recent calculations of electrostatic forces in frozen hexagonal arrays using a finite difference numerical solution of the Poisson-Boltzmann equation, with finite size ions and a detailed DNA structure derived from x-ray crystallography, provide even better agreement between theory and experiments and offer an explanation for the different force magnitudes observed with different cations (Sharp, 1993). For 0.4 M Na^+ and for the range of separations seen in Fig. 1, the calculated value of $\log(f_{e0})$ is 2.97, pleasingly close to the experimental value of 2.86 (a calculated reduced effective charge density of $\xi = 2.5$ versus the experimental 2.2). For the larger Cs^+ ion, both calculations and experiment give $\log(f_{e0}) = 3.22$ ($\xi = 3.2$).

The differences in force magnitudes between electrostatic and hydration repulsion are potentially instructive. As in the fluctuation-enhanced electrostatic force regime, the exponential prefactors, f_{h0}, in the high pressure regime depend on the counterion species bound to DNA. The differences among counterions in the two regimes, however, are not strongly interrelated. For example, there is about a factor-of-4 difference in hydration force magnitude at 28-Å separation between Li^+ and Cs^+. The difference between the same two ions is only a factor of 2 for inferred direct electrostatic repulsion or a factor of 1.5 for directly observed fluctuation enhanced electrostatic repulsion at larger spacings (Table 1). In 0.4 M salt, Li^+-DNA shows slightly (but consistently) stronger repulsion at low pressures than Na^+-DNA, but twofold weaker forces in the hydration dominated high pressure region. Lithium, the most strongly hydrated cation, confers on the molecule the weakest hydration force. We suggest that there is a kind of cancellation of hydration of the DNA phosphates by the binding cations. The cancellation is seen then as a weak net hydration of the ion-clad polyelectrolyte. The strength of the net hydration depends on the strength of the cation hydration.

Skewed rods

A new possibility is the ability to convert the force per unit length between parallel molecules into formulae that give the torque and the force between skewed rods. Again, simplifications have been made. Specifically, it is assumed that forces are additive, that segments of the two molecules interact independently so that the total interaction can be created as a sum in a new geometry. Such additivity is in keeping with the limits of second order perturbation theory used in order-parameter theories of forces and in the special case of that formalism that is the linearized form of electrostatic double layer interactions.

This electrostatic torque could play a significant role in polyelectrolyte assembly, especially for stiff polymer chains. It might be that one sees its action as one crosses the 30-to-35 Å "divide" between the bare and fluctuation-enhanced force regimes. Indeed, it is in this range of interhelical separations that a hexagonal-cholesteric transition has been located (Livolant, 1991; Durand et al., 1992). Our calculations also show (see above) that around $\leq$40 Å the electrostatic torque contributes significantly to the effective interaction of two skewed chains.

The incorporation of all these important details into a comprehensive theory of stiff polyelectrolyte liquid crystalline mesophases still seems quite far away, though significant progress in theoretical understanding of oriented polymers has been made in recent years (Selinger and Bruinsma, 1991; Kamien et al., 1992; Gupta and Edwards, 1993; Odijk, 1993). Continued experimental investigation of phase diagrams (Livolant, 1991; Durand et al., 1992), concurrent with measurement of the forces acting in biopolymer arrays, can provide a sound basis for quantitative thinking about stiff polymer organization.

We thank Theo Odijk, Kim Sharp, and Bruno Zimm for helpful comments.

REFERENCES

Anderson, C. F., and M. T. Record Jr. 1990. Ion distributions around DNA and other cylindrical polyions: theoretical descriptions and physical implications. *Annu. Rev. Biophys. Biophys. Chem.* 19:423–465.

Brenner, S. L., and V. A. Parsegian. 1974. A physical method for deriving the electrostatic interaction between rod-like polyions at all mutual angles. *Biophys. J.* 14:327–334.

Durand, D., J. Doucet, and F. Livolant. 1992. A study of the structure of highly concentrated phases of DNA by x-ray diffraction. *J. Phys. II (France).* 2:1769–1783.

Evans, E. A. 1991. Entropy-driven tension in vesicle membranes and unbinding of adherent vesicles. *Langmuir.* 7:1900–1908.

Evans, E. A., and V. A. Parsegian. 1989. Thermal-mechanical fluctuations enhance repulsion between bimolecular layers. *Proc. Natl. Acad. Sci. USA.* 83:7132–7136.

Fixman, M. 1979. The Poisson-Boltzmann equation and its applications to polyelectrolytes. *J. Chem. Phys.* 70:4995–5005.

Gupta, A. N., and S. F. Edwards. 1993. Mean-field theory of phase transitions in liquid-crystalline polymers. *J. Chem. Phys.* 98: 1588–1596.

Kamien, R. D., P. Le Doussal, and D. R. Nelson. 1992. Theory of directed polymers. *Phys. Rev. A.* 45:8727–8750.

Kornyshev, A. A., and S. Leikin. 1989. Fluctuation theory of hydration forces: the dramatic effects of inhomogeneous boundary conditions. *Phys. Rev. A.* 40:6431–6437.

Le Bret, M., and B. H. Zimm. 1984. Monte Carlo determination of the distribution of ions about a cylindrical polyelectrolyte. *Biopolymers.* 24: 271–285.

Leikin, S., V. A. Parsegian, D. C. Rau, and R. P. Rand. 1993. Hydration forces. *Annu. Rev. Phys. Chem.* 44:369–395.

Leikin, S., D. C. Rau, and V. A. Parsegian. 1991. Measured entropy and enthalpy of hydration as a function of distance between DNA double helices. *Phys. Rev. A.* 44:5272–5278.

Livolant, F. 1991. Supramolecular organization of double-stranded DNA molecules in the columnar hexagonal liquid crystalline phase: an electron

microscopic analysis using freeze-fracture methods. *J. Mol. Biol.* 218: 165–181.

Manning, G. S. 1978. The molecular theory of polyelectrolyte solutions with applications to the electrostatic properties of polynucleotides. *Quart. Rev. Biophys.* 11:179–246.

Odijk, Th. 1986. Theory of lyotropic polymer liquid crystals. *Macromolecules.* 19:2313–2329.

Odijk, Th. 1993. Personal communication.

Parsegian, V. A., R. P. Rand, N. L. Fuller, and D. C. Rau. 1986. Osmotic stress for the direct measurement of intermolecular forces. *Methods Enzymol.* 127:400–416.

Podgornik, R., and V. A. Parsegian. 1990. Molecular fluctuations in the packing of polymeric liquid crystals. *Macromolecules.* 23:2265–2269.

Podgornik, R., and V. A. Parsegian. 1992. Thermal-mechanical fluctuations of fluid membranes in confined geometries: The case of soft confinement. *Langmuir.* 8:557–562.

Podgornik, R., D. C. Rau, and V. A. Parsegian. 1989. The action of interhelical forces on the organization of DNA double helices: fluctuation-enhanced decay of electrostatic double-layer and hydration forces. *Macromolecules.* 22:1780–1786.

Rau, D. C., B. K. Lee, and V. A. Parsegian. 1984. Measurement of the repulsive force between polyelectrolyte molecules in ionic solution: hydration forces between parallel DNA double helices. *Proc. Natl. Acad. Sci. USA.* 81:2621–2625.

Rau, D. C., and V. A. Parsegian. 1992a. Direct measurement of the intermolecular forces between coounterion-condensed DNA double helices: evidence for long range attractive hydration forces. *Biophys. J.* 61:246–259.

Rau, D. C., and V. A. Parsegian. 1992b. Direct measurement of temperature-dependent solvation forces between DNA double helices. *Biophys. J.* 61:260–271.

Selinger, J. V., and R. F. Bruinsma. 1991. Hexagonal and nematic phases of chains. II. Phase transitions. *Phys. Rev. A.* 43:2922–2931.

Sharp, K. 1993. Personal communication.

Stigter, D. 1975. The charged colloidal cylinder with a Gouy double layer. *J. Coll. Interface Sci.* 53:296–306.

Tsao, Y.-H., D. F. Evans, R. P. Rand, and V. A. Parsegian. 1993. Osmotic stress measurements of dihexadecyldimethylammonium acetate bilayers as a function of temperature and added salt. *Langmuir.* 9: 233–241.

Wang, L., and V. A. Bloomfield. 1991. Small-angle x-ray scattering of semidilute rodlike DNA solutions: polyelectrolyte behavior. *Macromolecules.* 24:5791–5795.